

SOURCE MODELING OF THE 2018 LOMBOK EARTHQUAKE SEQUENCE ESTIMATED FROM THE EMPIRICAL GREEN'S FUNCTION METHOD

Aldilla Damayanti Purnama Ratri¹
MEE21701

Supervisor: Hiroe MIYAKE², Saeko KITA³

ABSTRACT

In 2018, a series of earthquakes in Lombok, Indonesia, occurred close together, causing a lot of casualties and property damage. To quantify the effect of the earthquake, we need to study source characteristics and conduct source modeling for these earthquakes. Therefore, we simulated the target event with strong motion data of the smaller event in the surrounding area, which have the closest hypocenter and similarity of focal mechanism to the target event using the empirical Green's function method. Then, we determined the parameters of source modeling, including source dimension ratio (N) and stress drop ratio (C) to conduct broadband ground motion simulation. After that, did a grid search calculation to get the best fit values for the strong motion generation area (SMGA). From the grid search, we obtain the best-fit SMGA size and the rupture starting point that can be used to capture the rupture propagation and aftershock directions for seismic hazard assessment. The SMGA size indicated that the western part of Lombok (the region of Mw 6.4 and 7.0) showed lower stress drop than the eastern part (the region of Mw 6.9) and all were still lower stress drops than the empirical relationship of the SMGA size to the seismic moment for crustal earthquakes. Furthermore, the relative SMGA locations indicate a relationship among the foreshock, the mainshock, and the largest aftershock that may trigger each other and have similar source characteristics with rupture directions.

Keywords: Earthquake, empirical Green's function, grid search, strong motion generation area

1. INTRODUCTION

The 2018 Lombok earthquake sequence started with Mw 6.4 at a shallow depth on 28 July 2018. In the same area, a more significant earthquake with Mw 7.0 occurred on 5 August 2018 and caused some casualties and damaging buildings. Another series of substantial earthquakes occurred on 19 August 2018 with Mw 6.9 striking the eastern part of Mw 7.0. Hereafter, we call the Mw 6.4 as the foreshock, the Mw 7.0 as the mainshock, and the Mw 6.9 as the largest aftershock. These earthquake sequences are categorized as crustal earthquakes that have shallow source faults. These earthquake sequences are located parallel to the Flores back-arc thrust. The Flores back-arc thrust is one of the major active faults in Lombok that extend westward from Flores Island (Hamilton, 1977, 1979; Silver et al., 1983). The detail of the tectonic setting of Lombok are shown in Figure 1. Lombok is one of the regions in Indonesia with a unique geotectonic position since the active tectonic plates surround the area in the four corners of the island. Regarding this, we try to know the characteristics of the earthquake in Lombok. Therefore, we simulated the target event with strong motion data of the smaller event in the surrounding area using the empirical Green's function method (EGFM). Then, we estimate strong motion generation areas

¹ Indonesia's Agency for Meteorology, Climatology, and Geophysics (BMKG), Jakarta, Indonesia.

² Associate Professor, Earthquake Research Institute (ERI), University of Tokyo.

³ International Institute of Seismology and Earthquake Engineering, Building Research Institute.

(SMGAs) to construct source modeling for the Lombok earthquake sequence and to know the stress drop.

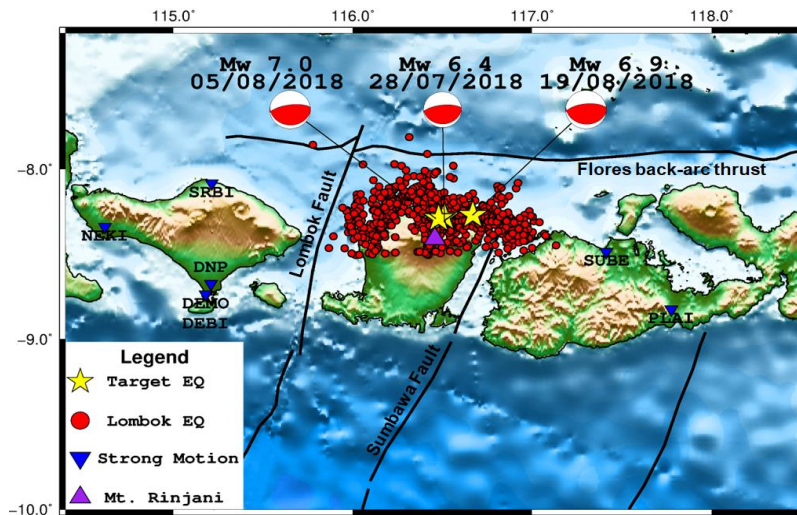


Figure 1. Tectonic setting of Lombok with earthquake sequences in 2018 with target events and strong motion stations.

2. DATA

To conduct broadband (0.1-10 Hz) ground motion simulation, we used the smaller event (foreshock or aftershock) that satisfy as an EGF event from the hypocenter and focal mechanism category. Therefore, we used earthquake data summarized in Table 1.

Table 1. Parameters of the target and EGF events used in this study

| No. | Date | Hypocenter location | | | Mw | Focal Mechanism | | | | Note |
|-----|------------|---------------------|----------|------------|-----|-----------------|------------|---------|----------|--------------|
| | | Lat (°) | Long (°) | Depth (km) | | Fault Plane | Strike (°) | Dip (°) | Rake (°) | |
| 1. | 28/07/2018 | -8.28 | 116.51 | 14.6 | 6.4 | FP 1 | 90 | 21 | 96 | Target event |
| | | | | | | FP 2 | 264 | 69 | 88 | |
| 2. | 29/07/2018 | -8.32 | 116.44 | 10.0 | 5.1 | FP 1 | 63 | 18 | 80 | EGF event |
| | | | | | | FP 2 | 254 | 72 | 93 | |
| 3. | 05/08/2018 | -8.29 | 116.47 | 17.6 | 7 | FP 1 | 96 | 21 | 103 | Target event |
| | | | | | | FP 2 | 262 | 70 | 85 | |
| 4. | 28/07/2018 | -8.28 | 116.51 | 14.6 | 6.4 | FP 1 | 90 | 21 | 96 | EGF event |
| | | | | | | FP 2 | 264 | 69 | 88 | |
| 5. | 19/08/2018 | -8.37 | 116.7 | 23.5 | 6.9 | FP 1 | 94 | 34 | 96 | Target event |
| | | | | | | FP 2 | 266 | 57 | 86 | |
| 6. | 19/08/2018 | -8.44 | 116.59 | 11.2 | 6.2 | FP 1 | 107 | 26 | 100 | EGF event |
| | | | | | | FP 2 | 276 | 65 | 85 | |

We also used the horizontal components of the strong motion data obtained from the stations of the Indonesia National Agency for Meteorology, Climatology, and Geophysics (BMKG). These stations have various accelerometers and digitizers with a sampling rate of 100 Hz. The detailed sensor locations and target earthquakes for this research are shown in Figure 1.

3. METHODOLOGY

3.1. Empirical Green's Function Method (EGFM)

Source modeling of these earthquakes is performed by the empirical Green's function method (EGFM). The EGFM is a method for modeling earthquakes using strong ground motion, which uses foreshock or aftershock related to a large earthquake as an empirical Green's function event (Irikura and Kamae, 1994). The main principle of the EGFM is using the smaller event that is close to the target (larger) event with a similar focal mechanism because the smaller event has already contained the information about the path propagation and local site effects that cover the velocity structure.

Then, to conduct source modeling, we need to do a waveform simulation by determining parameters for source modeling, including source dimension ratio (N) and stress drop ratio (C), which can be written as Eqs. (1-2):

$$N = fc_e / fc_t \quad (1)$$

$$C = \left(\frac{M_0}{m_0} \right) \left(\frac{fc_t}{fc_e} \right)^3 \quad (2)$$

Where N and C are the ratios of source dimensions and stress drops between large and small events, respectively. While, fc_t and fc_e is the corner frequency of the target and EGF events, respectively.

3.2. Grid search calculation

To construct the simulation using the EGFM, the dimension of length and width, the initial rupture position (subfault (i,j)) relative to the SMGA, the rise time, and the rupture velocity inside SMGA were set as search parameters. First, we determined the initial value of the element event size given as Eq. (3):

$$\text{Size of the element event} = 1 / fc_e * V_r \quad (3)$$

Where fc_e is the corner frequency of the EGF event in Hz and V_r is rupture velocity. In this research, the range of V_r is (0.6 – 0.9) of the shear velocity. Shear velocity depends on the depth of the target event. Then, we did a grid search calculation to get the best value for the SMGA parameters, including the size of the element event for the SMGA (length and width), the best position for the initial rupture (i,j) based on the selected strike and dip for each event, the rise time, and the rupture velocity inside the SMGA. To search the best solution for this, we need to consider the maximum correlation and minimum residual values between the observed and synthetic displacement waveforms.

4. RESULTS AND DISCUSSION

4.1. Estimation source parameters by EGFM

According to the calculation for source modeling parameter, waveforms for the target event are simulated using the EGFM, then comparing the observation and synthetic waveforms for horizontal components in acceleration, velocity, and displacement. The scaling parameters for source modeling and the best fit value for the SMGA parameters using grid search calculation are summarized in Table 2.

Table 2. Scaling parameter for source modeling and best fit values for SMGA.

| Parameter | Foreshock (Mw 6.4 paired to Mw 5.1) | Mainshock (Mw 7.0 paired to Mw 6.4) | Largest aftershock (Mw 6.9 paired to Mw 6.2) |
|----------------------------|---|---|--|
| Source dimension ratio (N) | 4 | 2 | 2 |
| Stress drops ratio (C) | 1.3 | 2.35 | 0.88 |

| | | | |
|---|---------------------------|-------------------------|----------------------------|
| Size of the element event for SMGA (km) | Length: 4.6 Width: 3.8 | Length: 16 Width: 15 | Length: 11.2 Width: 8.2 |
| Rupture starting point (i,j) | (2,1) | (1,1) | (1,1) |
| Rise time (s) | 0.21 | 0.84 | 0.6 |
| Rupture velocity (km/s) | 2.5 | 3.0 | 2.8 |

The foreshock modeling indicated that the area of the SMGA was the smallest. On the other hand, the largest SMGA was obtained for the mainshock event. Regarding the SMGA size for these events, the western part of Lombok (the area of Mw 6.4 and Mw 7.0) had a lower stress drop than the eastern part of Lombok (the area of Mw 6.9). We can see this in Figure 2, in which green and purple lines show the SMGA for the 2018 Lombok earthquake sequence. The green line represents the SMGA for Mw 7.0, 6.4, and 5.1, while the purple line represents the SMGAs for Mw 6.9 and 6.2.

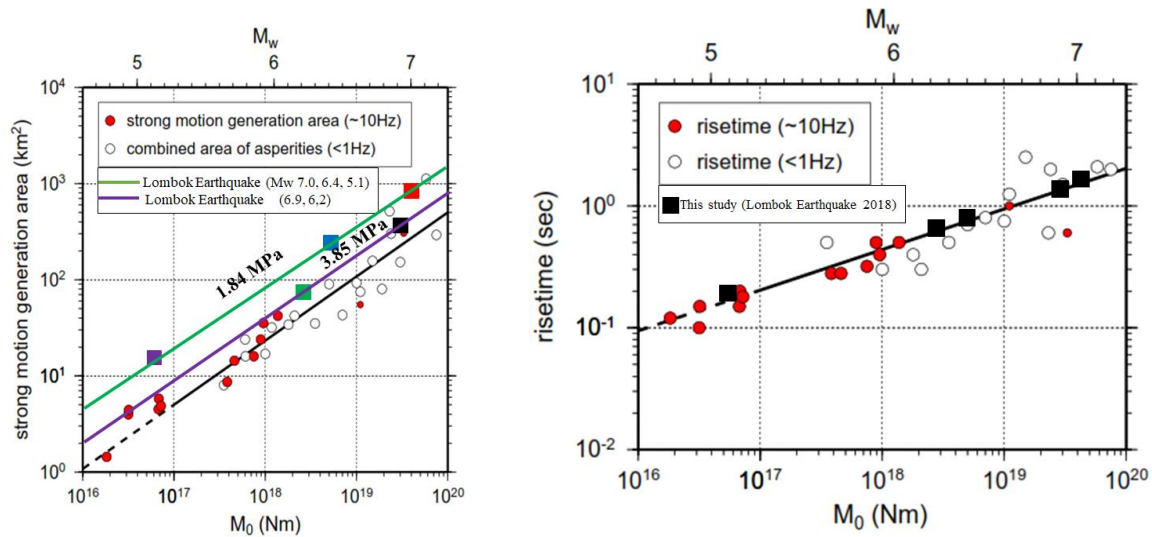


Figure 2. Scaling relationship between strong motion generation area and seismic moment (left) and between rise time and seismic moment (right). (Update from Miyake et al., 2003).

To validate the stress drop estimation based on the relationship of the SMGA and seismic moment, we calculated the stress drop for the 2018 Lombok earthquake sequence shown in Figure 2. We obtained that the stress drop for the mainshock was 1.84 MPa, but for the largest aftershock was 3.85 MPa. All of the stress drops were still lower stress drop than the empirical relationship of the SMGA size to the seismic moment for crustal earthquakes. This suggests the local stress drop variation in the Lombok region as well as the regional stress drop variation due to the tectonic setting. In addition, from Figure 2, we also see that the rise time for the 2018 Lombok earthquake sequence (black squares) is located in line with the black line. It means that the rise time for the 2018 Lombok earthquake sequence is similar to the rise time for the crustal event in the United States and Japan (Miyake et al., 2003).

4.2. Source modeling of the 2018 Lombok earthquake sequence

We conducted a source modeling (Figures 3 and 4) on the map based on the best fit value of the SMGA parameters obtained in Section 4.1 and selected strike and dip projected on the horizontal plane based on the dip direction. Figure 3 shows the sample modeling for the foreshock event (left) and the comparison of the observed and synthetic waveforms of acceleration, velocity, and displacement recorded at the TWSI station at subfault (2,1) (right).

Based on Figure 3 (left), the initial rupture starts at the red star, at the top left-hand of the SMGA, and extends radially toward the bottom right-hand direction (southeast direction) with 2.5 km/s

of the rupture velocity. The waves are well detected at the TWSI station because they are proportional to the direction of the rupture propagation. Therefore, the waveform at TWSI in Figure 3 (right) has a larger amplitude and narrower duration than other stations. It is possibly due to the directivity effect.

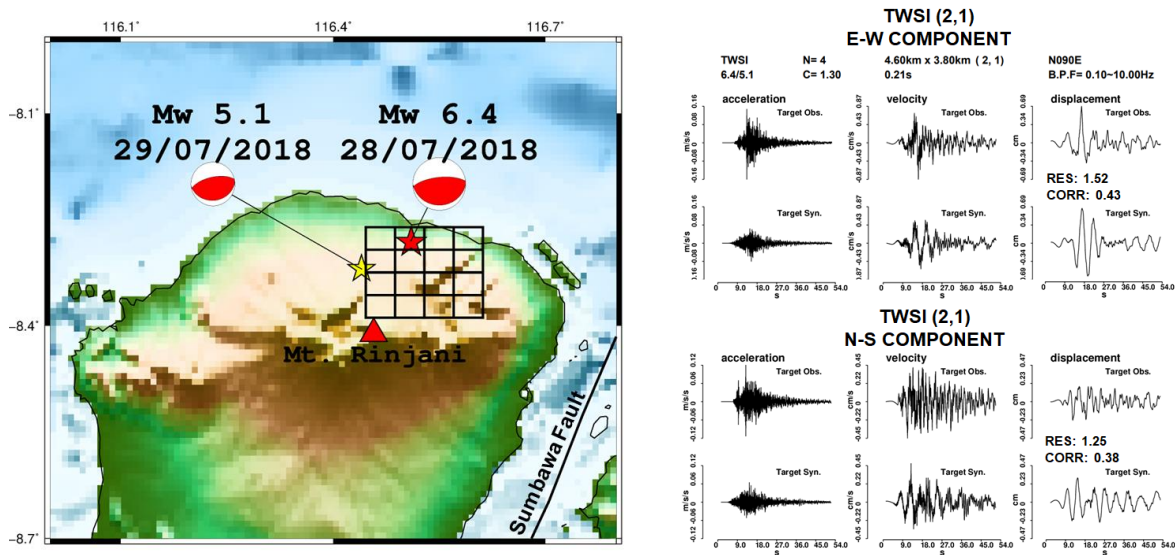


Figure 3. The foreshock source modeling (left) and the comparison of the observed and synthetic waveforms of acceleration, velocity, and displacement recorded at the TWSI station (right).

As seen in Figure 3, we also conducted source modeling for the mainshock and the largest aftershock. We obtained that the rupture location for these targets started at a similar position and had the same rupture propagation direction (Figure 4). The position dominated at the shallow northwestern corner of the SMGA and extended radially toward the southeast down dip direction.

Based on the evaluation of the rupture propagation and the SMGA size for each event, we obtained a relationship between the foreshock, the mainshock, and the largest aftershock. The foreshock event may trigger the mainshock, and the mainshock event may trigger the largest aftershock. Therefore, these Lombok sequences shared similar source characteristics.

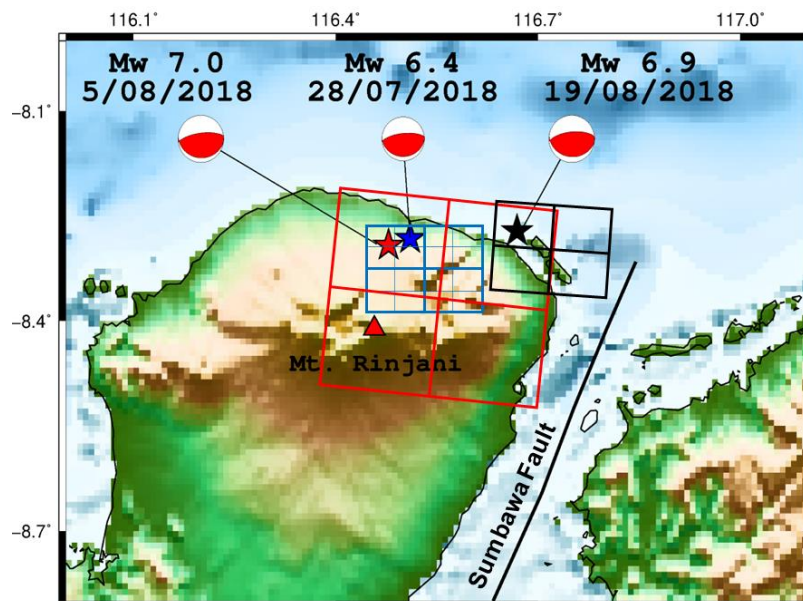


Figure 4. Combination of three source modeling for the target earthquakes in the 2018 Lombok earthquake sequence. The star and the rectangle respectively represent the hypocenter and the SMGA for the foreshock (blue), the mainshock (red), and the largest aftershock (black).

5. CONCLUSIONS

The series of the Lombok earthquakes that occurred from July to August 2018 have unique characteristics due to the source heterogeneity in different tectonic settings over the world. To understand the source characteristics of these earthquakes, we conducted the simulation and modeling using EGFs for the foreshock with Mw 6.4, the mainshock with Mw 7.0, and the largest aftershock with Mw 6.9. We selected one earthquake to be an EGF event that satisfies the requirements, including the focal mechanism and hypocenter very close to the target event.

The foreshock modeling indicated the smallest SMGA. On the other hand, the largest SMGA was obtained for the mainshock event. Regarding the SMGA size and rise time for these events, the western part of Lombok (the region of Mw 6.4 and Mw 7.0) had a lower stress drop than the eastern part of Lombok (the region of Mw 6.9). All were still lower stress drops than the empirical relationship of the SMGA size and rise time to the seismic moment for crustal earthquakes. This suggests the local stress drop variation in the Lombok region as well as the regional stress drop variation due to the typical tectonic setting of the target region.

The rupture for these targets started at a similar position and had the same rupture propagation direction. The position dominated at the shallow northwestern corner of the SMGA and extended radially toward the southeast downdip direction. Finally, from examining the rupture propagation and SMGA size for each event, we obtained a relationship among the foreshock, the mainshock, and the largest aftershock. The foreshock event may trigger the mainshock, and the mainshock event may trigger the largest aftershock. Therefore, these Lombok sequences shared similar source characteristics.

ACKNOWLEDGEMENTS

This research was conducted during the individual study period of the training course “Seismology, Earthquake Engineering and Tsunami Disaster Mitigation” by the Building Research Institute, JICA, and GRIPS. I would like to express my sincere gratitude to my supervisor Dr. Hiroe Miyake for her valuable support and experience which helped me to complete my research successfully, and to Dr. Saeko Kita for her guidance and advice during my individual study. I would also like to acknowledge Dr. Takumi Hayashida and Dr. Tatsuhiko Hara for their permanent support from the beginning to the end of the program. I would also like to express thankfulness to Ariska Rudyanto, S.Si, Dipl. Tsu, M.Sc and Angga Wijaya, S.Tr for their data support and processing during my individual study.

REFERENCES

- Hamilton, W, 1977, Subduction in the Indonesian region. In island arcs, Deep sea trenches and back-arc basins (eds M.Talwani and W.C.Pitman), <http://doi.org/10.1029/ME001p0015>.
- Hamilton, W, 1979, Tectonic of the Indonesia region, *Geol. Soc. Malays. Bull.* 6, 3-10.
- Irikura, K., & Kamae K., 1994, Estimation of strong ground motion in broad-frequency band based on a seismic source scaling model and an empirical Green's function technique, *Ann. Geofis*, 37, 1721-1743.
- Miyake, H., Iwata, T., & Irikura, K., 2003, Source characterization for broadband ground-motion simulation: Kinematic heterogeneous source model and strong motion generation area, *Bull. Seismol. Soc. Am*, 93, 2531-2545.
- Silver, E.A., Reed,D., & McCaffrey, R., 1983, Back-arc thrusting in the Eastern Sunda Arc, Indonesia: A consequence of arc-continent collision, *J. Geophys. Res.* 88, 7429.